ADVANCED INTELLIGENT SYSTEMS
Open Access
www.advintellsyst.com

A Soft Pneumatic Exosuit to Assist Pronosupination in Individuals with Spinal Cord Injury

*Roberto Ferroni, Gaetano D'Avola, Daniele Filippo Mauceri, Chiara Pau, Giorgia Sciarrone, Gabriele Righi, Jacopo Carpaneto, Marta Gandolla, Giulio Del Popolo, Silvestro Micera, and Tommaso Proietti**

Forearm pronosupination is an essential movement for many activities of daily living as it complements hand manipulation. Despite being highly impaired in individuals with spinal cord injury (SCI), it is rarely assisted by wearable robots, likely due to the challenging anchoring to the body and the risk of hindering hand capabilities. Here, a lightweight (30 g) soft wearable robot is introduced to assist pronosupination, employing a pneumatic fabric-based actuator that twists around the forearm, without impeding hand movements. It is mechanically transparent when unpowered but generates up to 122 N of force when inflated at low pressure (70 kPa). The device is tested on 10 SCI individuals, showing significant improvements in range of motion and reduced muscular effort. Additionally, participants engage in a target-hitting exergame, achieving higher scores and enhanced performance when assisted. The design potentially ensures compatibility with other wearables, showing promise for integrated upper limb assistance in individuals with neurological conditions.

1. Introduction

A spinal cord injury (SCI) is a devastating trauma—often traumatic and in young adults—causing partial or complete loss of sensory and motor function below the injury level.[1] SCI imposes a severe physical, psychological, and financial burden on patients and their families, with similar incidence across continents (54 cases per million in the US, 66.4 in China, 77.8 in Germany, and 32.3 in Australia).[1] Cervical SCI—injury occurring at the cervical portion of the spine, C1–C7—accounts for 47.2% of traumatic SCI cases, often causing tetraplegia and life-threatening symptoms that interfere with activities of daily living (ADLs).[2] Unsurprisingly, individuals with cervical SCI value restoring arm and hand function, even partially, as their highest priority for improving their quality of life.[3]

Regardless of the impairment level, SCI individuals need external assistance to compensate for their deficits. While promising, most technological approaches are not yet viable solutions (e.g., electrical stimulation):[4,5] restoring arm and hand motor function in high-level spinal cord injuries remains elusive, requiring the challenging coordination of multiple muscles across joints (shoulder, elbow, wrist, and hand).[6] Robotics, including wearable exoskeletons, has shown promise to tackle multi-joint assistance, but only a limited number of devices have progressed to clinical testing for SCI or other neurological conditions.[7] When focusing on distal joint assistance, we observe a large amount of research targeting hand opening–closing support.[8–11] Forearm pronosupination critically affects the execution of many ADLs, such as eating with a fork, opening a bottle, pouring water inside a glass, or turning a doorknob, and naturally complements the capability of the hand. However, robotic devices addressing assistance to this degree of freedom (DOF) lack in literature. This is

R. Ferroni, G. D'Avola, D. F. Mauceri, C. Pau, J. Carpaneto, S. Micera, T. Proietti
The Biorobotics Institute and Department of Excellence in Robotics & AI
Scuola Superiore Sant'Anna
Pisa 56127, Italy
E-mail: tommaso.proietti@santannapisa.it

G. Sciarrone, G. Righi, G. Del Popolo
Spinal Unit
Careggi University Hospital
Firenze 50139, Italy

The ORCID identification number(s) for the author(s) of this article can be found under https://doi.org/10.1002/aisy.202500124.

DOI: 10.1002/aisy.202500124

D. F. Mauceri, M. Gandolla
Department of Mechanical Engineering
Politecnico di Milano
Milano 20156, Italy

S. Micera
Translational NeuroEngineering Laboratory
Neuro-X Institute
School of Engineering
École Polytechnique Fédérale de Lausanne (EPFL)
Lausanne 1015, Switzerland

S. Micera, T. Proietti
Modular Implantable Neuroprostheses (MINE) Laboratory
Università Vita-Salute San Raffaele
Milano 20132, Italy

likely due to the complex anchoring of the robot to the human arm to actuate this DOF, which often hinders the ability to grasp an object, as most of the examples in literature require grasping a handle.[12–16]

The limited number of designs that have been proposed to support pronation and supination of the forearm were mostly validated on few healthy individuals, thus not making the leap to the real use case.[17–19] Those studies reaching clinical validation, instead almost exclusively focused on post-stroke rehabilitation through rigid end-effector-like robots.[12,13,20–34] Catàlan et al. showed notable results using a portable, wheelchair-mounted exoskeleton and a brain–computer interface, that assisted multiple joints in the upper limb (including pronosupination) of 10 neurologically impaired patients (including SCI) during ADLs.[35]

From a technical standpoint, all these devices can output a considerable torque, produce range of motion (ROM) that are compatible or even larger than the biological requirement, and can detect the user's movement intention through electromyography,[18,36] electroencephalography,[37] or force sensors.[38,39] The vast majority is electrically actuated, requiring rails or rotation gears around the arm, that limit the device's compactness (a few hundred grams, acting directly on the arm). In addition, a good amount of them is equipped with graphical user interfaces aimed at making the training more engaging by means of exergames.[13,15,16,23,26]

In more recent works, research started emphasizing on lightweight designs and portability as crucial features in the perspective of an assistive paradigm, potentially unsupervised at home. For example, Su et al.[40] demonstrated a cable-driven wearable skin brace tested on 3 stroke individuals, and later evaluated the feasibility (on 4 healthy participants) of a similar approach, combined with a glove exosuit, aiming at expanding the hand grasping support over multiple forearm orientations.[41] Balasubramanian et al.[42] and Das et al.[43] instead used pneumatic artificial muscles (PAMs) to assist repetitive therapeutic tasks in healthy individuals. Realmuto et al. proved the effectiveness of a fabric-based pneumatic orthosis, both in healthy[44] and in children with cerebral palsy,[45] showing reduced effort in tracking a reference trajectory. Jeong et al.[46] proposed a wearable robot actuated by shape memory alloys (SMAs), demonstrating enhanced pronosupination by $<16°$ in 4 patients with stroke. Park et al.[47] proposed an interesting design using a fabric-based soft sleeve that can support pronation or supination. Even though this design was not evaluated neither on healthy individuals nor or patients, they showed that it can provide 70 N in traction force and 0.7 Nm torque when actuated at 50 kPa.

Here, we propose the design of a novel wearable robot that actively assists the forearm pronation and supination, with a soft and portable design that does not hinder hand grasping movements, see **Figure 1**. The robot is pneumatically actuated, with thermoplastic polyurethane (TPU)-coated nylon air chambers twisting along the forearm. This structure makes the device very lightweight (30 g considering the worn portion only). Supplementary Video S1, Supporting Information shows the donning of the robot and its working principle. Earlier soft designs are innovative, yet each carries a limiting trade-off: cable-driven cuffs are thin but still add >130 g to the limb;[40] lightweight pneumatic sleeves either require high pressures (>400 kPa)[45] or, while being promising, have not yet been tested on human and lack data about comfort (i.e., maximum thickness when inflated);[47] PAM-based devices, as the one suggested by Das et al.[43] remain quite bulky and weigh more than 390 g; and the SMA-based wearable proposed by Jeong et al.[46] exceeds 1.5 kg and operates at skin-side temperatures of ≈65 °C.

By contrast, our textile actuator delivers clinically relevant torque at only 70 kPa, adds <50 g to the limb, all while leaving the hand free. In this work, not only did we introduce the design of the robot and its mechanical characterization—including mechanical transparency validated on 5 healthy participants—but we also assessed the robot-assistive efficacy by testing on 10 people surviving a cervical SCI. We quantified this assistance both in terms of ROM and reduction of muscular activity through a target-hitting exergame that was purposely developed for this work (a classic Whac-A-Mole). Importantly, while the robot can support both pronation and supination, our analysis focused on supination as our participants (mostly all with C3–C4 lesions) generally lacked active control of this movement. Indeed, higher cervical lesions impact the musculocutaneous nerve that acts on the biceps and supinator, while lower lesions (level C6–C7) impact the median nerve, acting on the pronator muscles.[48] Assistive pronation was therefore not tested in our pool of SCI participants. However, the design is symmetrical for both movements—the actuator needs to be attached to the palm of the hand, instead of the back of the hand, and twisted around the arm in the opposite direction of the supination—and we expect a similar behavior in terms of performances. An interesting and promising feature of the design is that its lightweight and slim profile has potential for seamless integration with many existing wearable solutions (e.g., traditional rigid exoskeletons), potentially augmenting their range of action.

2. Results

We recruited 5 healthy individuals (2 males, 3 females; 27.6 ± 2.3 years old; weight, 63.8 ± 16.3 kg; height, 174.2 ± 12.9 cm) and 10 SCI individuals (10 males with a lesion between the C3 and C7; 2 motor complete lesion; 54.3 ± 11.9 years old; weight, 82.3 ± 12.4 kg; height, 178.7 ± 5.9 cm) to participate in a single-session data collection using the proposed soft robot. Individual data are available in Table S1, Supporting Information. After characterizing the actuator mechanically using a universal testing machine, the healthy participants performed a transparency test, without wearing and wearing the robot powered off. Then, a test of active ROM was also performed by the SCI participants, before engaging with the custom exergame for 2 min. All tests involving the SCI participants were performed in two conditions—robot *off* and robot *on*—with randomization between the participants.

2.1. The Soft Actuator Can Produce up to 122 N at Low Pressure, While Being Mechanically Transparent when Powered Off

The results of the mechanical characterization of the actuator at the universal testing machine are shown in **Figure 2**. As the device is pressurized, each fabric chamber—sub-millimeter thickness when uninflated—expands to only about 20 mm at 70 kPa pressure because the TPU-coated nylon fabric composite is essentially inextensible in plane, this slight volume growth is accompanied by a decrease in chamber width (Figure S2c, Supporting Information), generating axial shortening that is

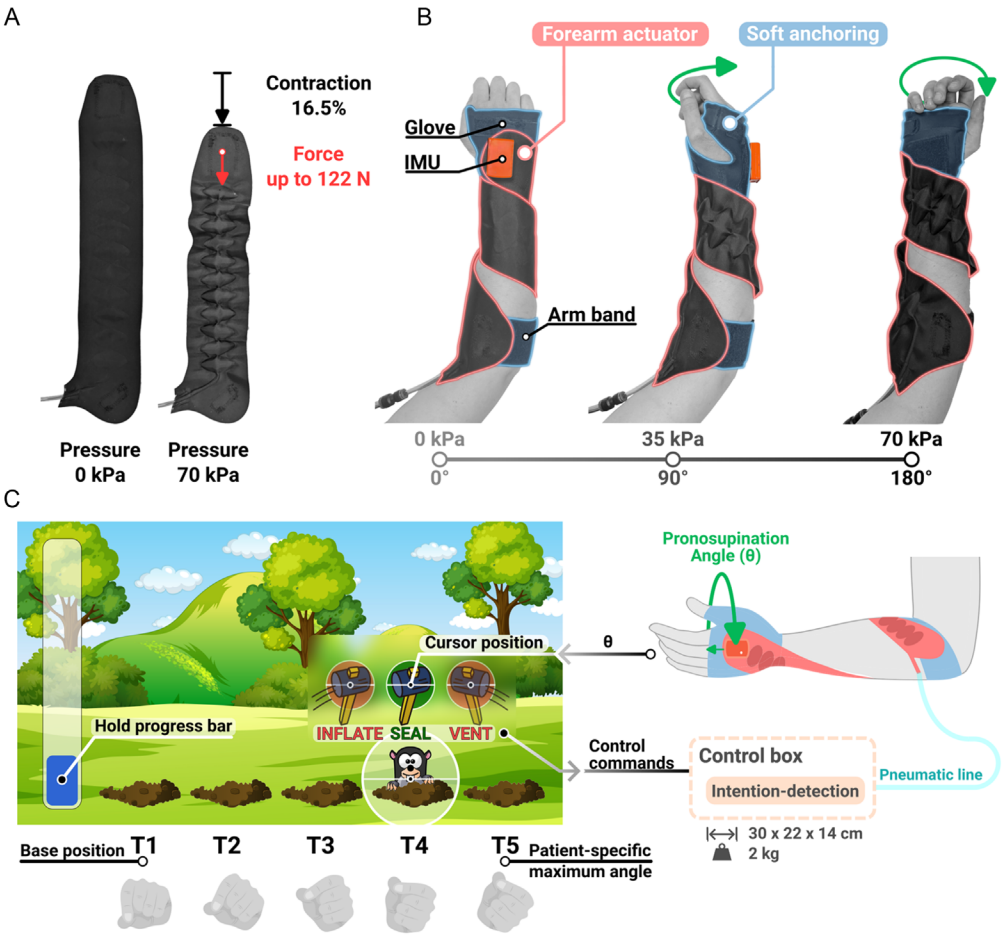

Figure 1. Overview of the forearm soft robot, including the target-hitting exergame. A) The soft actuator vented (left, 0 kPa) and at maximum pressure (right, 70 kPa). When unconstrained, inflation to 70 kPa induces a contraction of 16.5% relative to resting length. When fully extended (0% CR), the actuator can generate tensile forces up to 122.6 N. The shown actuator measures 44 cm with 11 air chambers of 5 cm width, but it can be easily customized to the body characteristics of the user (time to manufacture below 10 min). B) Working principle of the forearm robot (supination mode). By inflating, the actuator generates a torque, causing the rotation of the forearm. The actuator is worn around the forearm using Velcro straps, attached both distally to a neoprene hand brace, and proximally to a neoprene armband, positioned just above or below the elbow, depending on forearm length. An IMU is attached to the wrist and measures the forearm pronosupination angle. C) Overview of the target-hitting exergame (Whac-A-Mole). On the left, the graphical interface that was shown to the participant, which comprises 5 target positions (T1–T5) represented by dens; the target (the mole) appears randomly in one den at a time. The participant controls the horizontal position of the cursor (the hammer) by changing the forearm angle (measured by the IMU). In the assisted condition, the participant initiates the movement at their own pace as soon as the target appears, with the control algorithm detecting motion based on a customizable threshold for forearm rotation velocity. Once detected, the actuator assists in reaching and holding the target. To score a point, the hammer must be held over the mole for 1 s (minimum hold time). The blue progress bar provides visual feedback about the hold time for scoring a point. The cursor's position relative to the target is used to command the robot (inflate, vent, and close) in the assisted condition, supporting the participant in reaching and maintaining the target.

additive across the serially connected chambers. The soft actuator can produce a remarkable traction force of 122.6 ± 1.16 N at a relatively low pressure of ≈70 kPa, when in a full extended configuration (0% contraction ratio (CR)). A first-order least-square fit confirmed that the force–pressure relationship is strongly linear (mean R^2 across the tested CRs = 0.97), thus the total traction of the eleven air chambers can be taken as the sum of the identical single-chamber contributions. When using these values in a simplified model of the interaction between the robot and the human forearm (male, 1.85 m height, body mass index 23, see Figure S1, Supporting Information), we estimated 2.2 Nm of max torque production (again, when fully pronated). Despite these high force/torque values, when powered off, the actuator is mechanically transparent i.e., it does not interfere with natural movements (see **Figure 3**). Not only kinematically (no significant reduction in ROM when powered off vs. when doffed, $p > 0.05$), but also from a muscular activity standpoint (no significant increase in EMG at the biceps or pronator teres, $p > 0.05$). This is due to the lightweight nature of the actuator and its textile-based structure.

2.2. The Soft Robot Enhanced Active ROM and Reduced EMG Activity in Individuals Suffering Cervical SCI

While mechanically transparent when powered on, the soft robot can enhance active ROM and simultaneously induce the reduction of muscle activity as measured by EMG. This is shown in Figure 3,

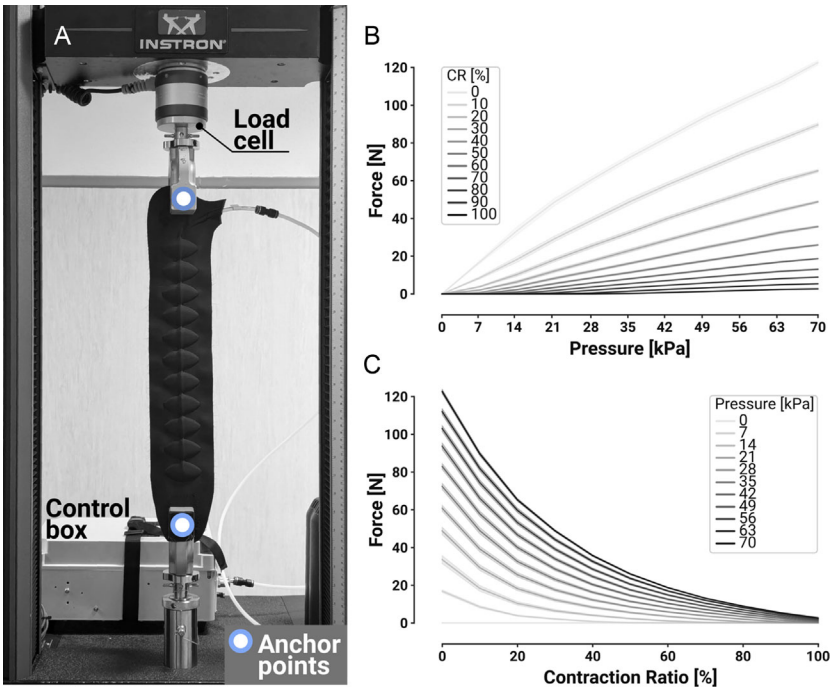

Figure 2. Mechanical characterization of the soft actuator. A) The soft actuator mounted into a universal testing machine (Instron 5965, Instron Corporation, USA). The eleven air chambers are clearly visible in the picture. As they pressurize, their volume increases while their width reduces, causing a contraction over the whole actuator and thus a vertical pulling force. B) The quasi-linear force-pressure relation at given CRs. The actuator can produce 122.6 ± 1.16 N at 70 kPa, from a full extended configuration. C) The non-linear force–CR relation at set values of pressure.

with data from the 10 SCI participants. We observed +31.7% improvement in active ROM (with the passive-triggered control) from ≈71.6° of supination to 94.2 when supported ($p < 0.01$). At the individual level, apart from one participant who was able to achieve almost 150° of supination unsupported, all of them improved their ROM. The increase of ROM came together with a significant reduction of 45.4% in the activity of the biceps muscle ($p < 0.05$), mainly responsible for the supination movement. As expected, the pronator teres, mostly responsible for pronation, did not differ significantly in the two conditions. Importantly, the values of maximum ROM for each participant were then used to calibrate the exergame, that was thus customized for each participant and for each condition (*robot off*, *robot on*).

2.3. Playing a Target-Hitting Exergame, SCI Individuals Improved Their Performance Due to the Soft Robot

When engaged in the target-hitting exergame, SCI individuals improved their performance, both at individual and group level when assisted by the supination robot. As confirmation of what is shown in Figure 3, we observed an increased ROM during the game, too. Importantly, this did not come at the expense of a worse time to target (no significant difference in the time elapsed to reach the target angle between *off* and *on* conditions), nor to muscular activity (no significant difference in biceps or pronator teres EMG between *off* and *on* conditions, see **Figure 4**). This is particularly significant considering that by calibration, the targets in the *on* condition were placed at larger angles and thus, further distance ($\theta_{\max}$ assisted $> \theta_{\max}$ unassisted).

Improvements were also observed when analyzing the game-related metrics, such as the number of hit targets (+10.8%, **Figure 5**a), with 6 out of 10 participants who improved their score and 2 who scored equally in the two conditions (see Figure 5b). Hold time (time over the target before granting the point) improved significantly in one target only (T4, see Figure 5a). We observed potential learning effects in few participants with reduced hold time as they were playing the exergame, as shown in Figure 5c.

3. Discussion

Forearm pronosupination is a critical movement that naturally complements hand manipulation in the execution of many activities of daily life. This motion is often impaired in individuals with neurological conditions, such as cervical SCI. However, designing wearable robots to assist this joint is challenging; consequently such devices are rare in literature.

Supplementary Table S2, Supporting Information collates studies, presenting a total of 32 devices reported since 2003 targeting the forearm pronosupination, either exclusively or as one of the other DOFs assisted by the robotic system. Solutions that have been validated on at least one participant have been reported. Among these, the vast majority (84%) consists of rigid robotic systems (i.e., end effector-type robots (28%),[20,26,29] exoskeletons or powered orthoses (50%),[25,32,49–52] robotic rehabilitation platforms (22%)).[15,16,53,54] These devices appear much more powerful from a mechanical performance standpoint, as they can output way larger torques compared to the human joints' biological needs:

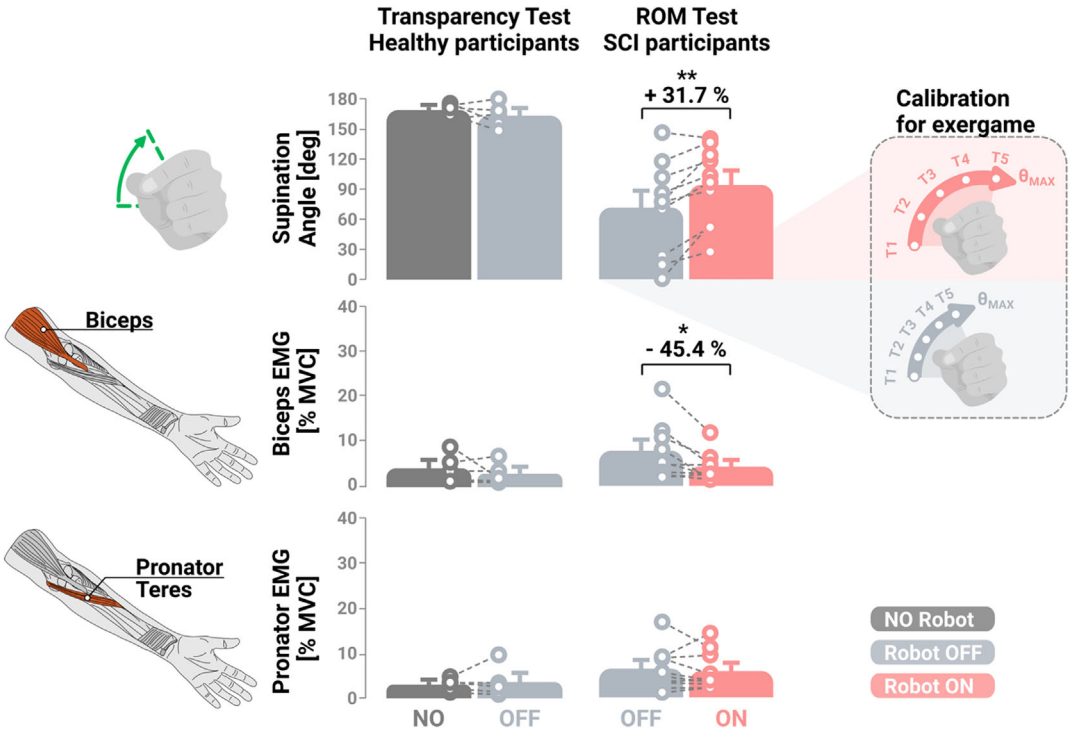

Figure 3. Transparency test with healthy participants and active ROM test with SCI participants. The soft actuator resulted in mechanically transparent, not interfering with the natural ROM of the user when powered off. This was validated, both from a kinematic (no significant reduction in supination angle) and a muscular activity point of view (no significant reduction in biceps or pronator teres EMG). When powered on, instead, the robot was able to enhance the ROM of the 10 SCI participants (+31.7%, $p < 0.01$), as well as reduce the biceps activity (−45.4%, $p < 0.05$), which is the main responsibility of the supination movement. As shown in the dashed gray box, for each participant, the max ROM reached in each condition was used to calibrate the exergame before starting the 2-min session. Finally, a threshold on the forearm rotation angular velocity was adjusted to detect the patient's movement intention, that triggered the robotic assistance.

for instance, compared to the normative joint torque required for a healthy human being to carry ADLs (estimated around 0.06 Nm for the forearm pronosupination motion),[55] on average end effector-type robots are capable of outputting 9.8 Nm, rehabilitation robotic platforms 3.2 Nm, exoskeleton frames 2.7 Nm. Some rigid devices were used in clinical studies which proved that robotic-assisted therapy is a viable option to traditional stroke rehabilitation, showing significant clinical improvements of reduced spasticity,[20] improved standard clinical assessments, such as Fugl–Meyer Score,[13,27,49] or increased maximal voluntary strength in forearm supinator muscles.[56] Also, similar technology has been preliminarily used with other neurological conditions such as Parkinson's disease[28] or SCI ($N = 1$ incomplete cervical SCI using the RiceWrist exoskeleton[32] or the RiceWrist-S).[57]

However, weight and size are still limiting factors when discussing rigid exoskeletons' accessibility. There are some exceptions, as for the case of portable rehabilitation robots which still require help to be carried around, but indeed provide valuable contribution for forearm or wrist training, that has been shown to result in not significantly different rehabilitation outcomes compared to a multijoint functional rehabilitation program.[56] These weigh on average around 5 kg and are table-top solutions. Also, some wearable rigid exoskeletons achieved a remarkably low weight (SUE 0.56 kg,[50] MAHI-EXO II 0.34 kg,[51] SpringWear 0.5 kg),[34] but only one device has been evaluated in unstructured settings.[58] Interestingly, in a recent survey,[59] individuals living with impaired hand functionality considered 200 g of additional mass onto their hand as a manageable load and would feel a thickness superior to 3 cm on the back of their hand as too bulky. These requirements set challenging thresholds for most robotic systems.

Factors such as comfort, portability, form factor, and weight, pushed the development of assistive devices towards more soft devices: the first one supporting pronosupination (together with hand open/close DOF) dates back to 2018 (ForceHand Glove).[43] These pose other challenges, starting from their mechanical characterization which is often not reported (only three out of the five gave a measure of delivered torque).[40,44,46] This is likely due to harder modeling and thus, the need to experimentally characterize the performance of the robots, without the possibility to derive it from the motors' specifications and the transmission design choices. Notably, the usually much lower weight reported for these robots (395 g on average) is related to only reporting the actuator's weight, excluding the actuation unit. Only one group included the weight of the whole wearable system, which comprised a backplate housing microcontroller, motors, and battery (1.3 kg).[60] Moreover, only few systems have been validated on healthy individuals, and even less tested on patients in clinical settings (9 stroke,[60] 7 children with CP,[45] 3 stroke,[40] and 4 stroke).[46]

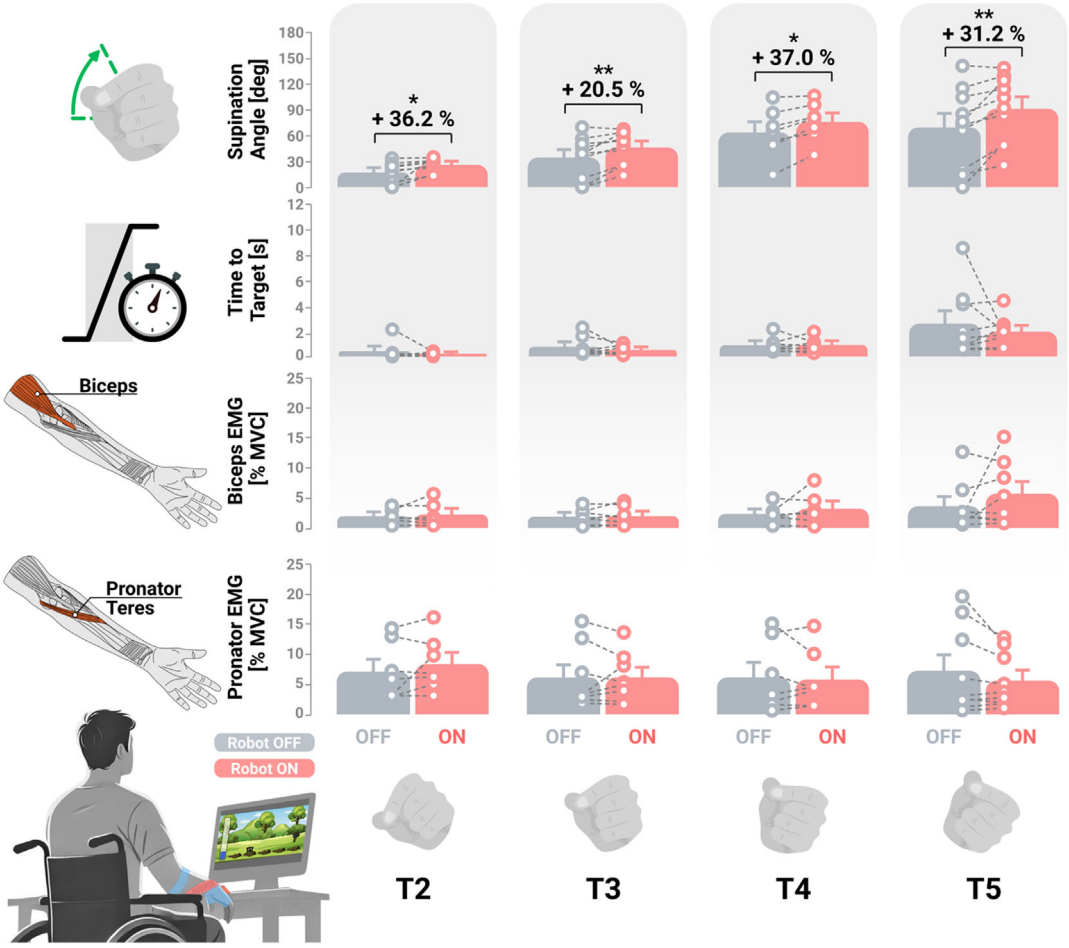

Figure 4. Kinematics and muscular activity during the 2-min exergame. The bar plots show target-dependent (T2–T5) metrics (supination angle, time to target, normalized biceps EMG, and normalized pronator teres EMG) in both, unassisted (OFF) and assisted (ON) conditions. In the assisted condition, we observed larger supination angles for each target (T2, +36.2%, $p < 0.05$; T3, +20.5%, $p < 0.01$; T4, +37.0%, $p < 0.05$; T5, +31.2%, $p < 0.01$). Although the targets were placed at greater angular distances, this did not affect the time to target ($p > 0.05$) nor the muscles' activity ($p > 0.05$).

Here, we introduced and demonstrated a new soft robot for assisting the forearm movements by means of a textile-based pneumatic actuator. Depending on the anchoring to the arm, the robot engages one joint rotation or the other, thus pronation or supination. However, due to the specificity of the participants of this study, we mainly focused on the supination movement, as much more affected.

We first showed that the textile-based design naturally provides the device with mechanical transparency, as demonstrated by the healthy individuals not reducing their ROM or increasing their muscular activity while using the robot in a powered off condition. This is not only a distinct characteristic and advantage of soft wearable robots over traditional rigid counterparts,[61,62] but also a highly desirable feature for quantitatively monitoring human movement, enabling unobtrusive assessments during use.[63] Then, we assessed the effectiveness of the support by the robot on 10 individuals suffering from cervical SCI. We showed that the robot can amplify the residual ROM of these people (+31.7%) while also reducing the required muscular effort on the biceps muscle, selected to better describe the supination movement through surface EMG recordings (−45.4% with respect to the maximum voluntary contraction, MVC). As expected, no reduction was observed on the pronator teres which is, instead, mostly responsible for pronation movements. The concurrent increase of ROM and decrease of EMG activity is the result of the control strategy, as an increased ROM would normally cause an increased EMG activity too. The robot was indeed controlled by a passive-triggered strategy, engaging the user to initiate the movement to start the inflation of the actuator and thus the assisting torque. Noticeably, for most of the participants, the achieved ROM was closer to the minimum pronosupination angle necessary to perform common ADLs (40°–140°),[64] which underline the effectiveness of the robot. Seven patients out of 10 reached an angle around 90° or above, which is sufficient to assist common ADLs such as feeding, or using a smartphone.[65] Despite improving (at least doubling their ROM when assisted), this was not the case for the three other participants (S4, S5, S9), who had particularly low baseline ROM (<25°). However, to boost up the support by the robot, we could increase the number of air chambers on the actuator, and thus the number of turns around the

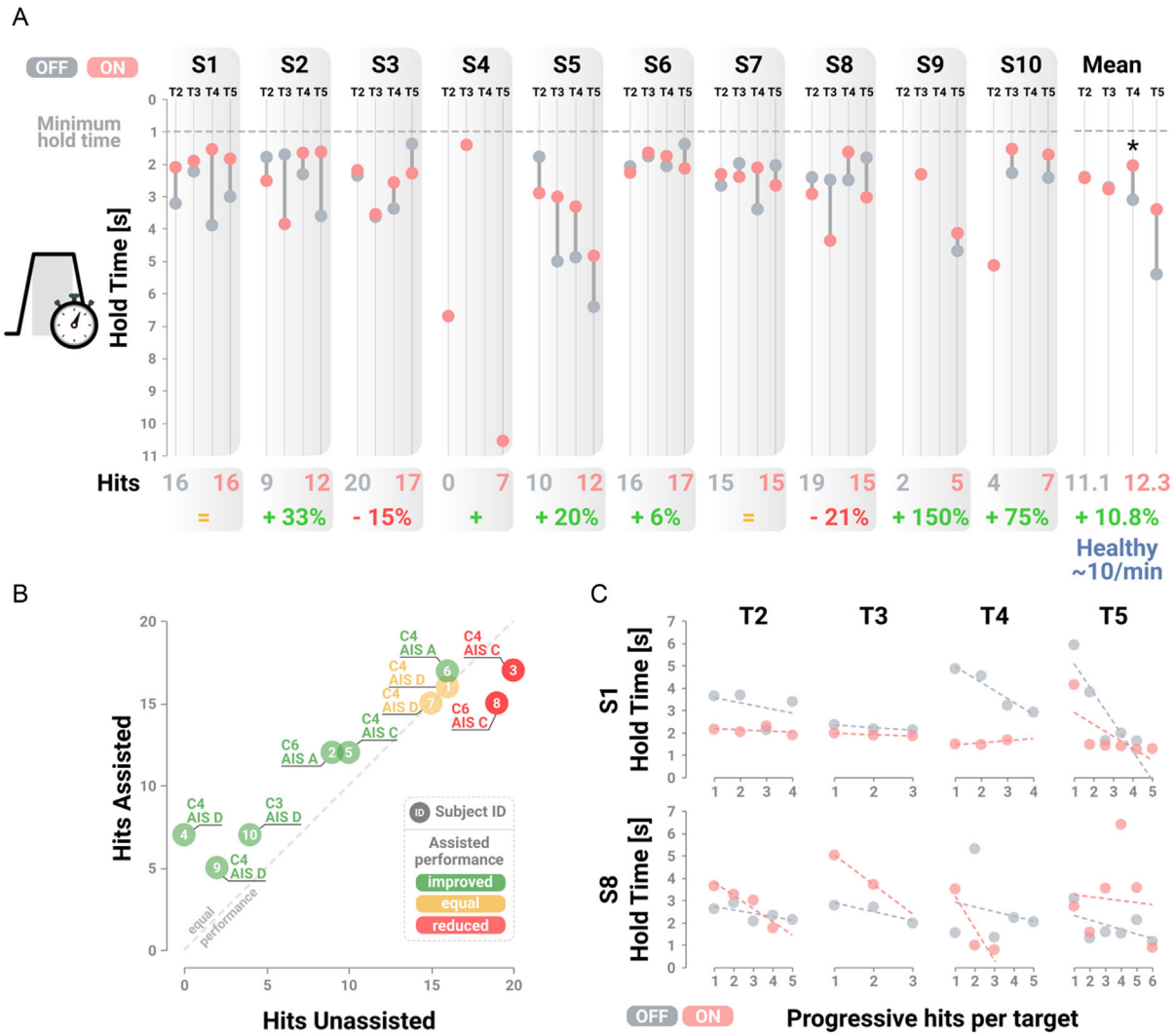

Figure 5. Performance-related metrics during the 2-min exergame. A) For each SCI patient, the time elapsed on average over each target (hold time, T2, T3, T4, T5) before scoring the point, both in the unassisted (OFF) and assisted (ON) conditions. The minimum hold time (1 s) is shown with a dashed line. Six patients out of 10 improved their scoring, while 2 reduced their performance when assisted by the robot. On average, participants improved their scoring significantly (+10.8%, 11.1 not assisted vs. 12.3 assisted). Noticeably, healthy participants scored 10 hits min^{-1} on average, regardless of the condition (assisted or unassisted). B) Comparison of the hits by each patient in both unassisted and assisted conditions. The dashed diagonal line represents an equal hit count for the two conditions. Text labels aside each subject marker indicate their injury level and AIS score. The only two participants who reduced their scores were the two hitting the largest number of targets unassisted (meaning the ones with the best baseline ROM). C) Learning effect across target-hitting repetitions for two exemplar subjects (S1 and S8). Each subplot shows hold time for one target (T2–T5) as a function of the progressive hit number. These two participants were selected because they scored ≥3 hits on every target in both conditions, enabling meaningful linear regression of the available observations (shown as dashed lines, for each target and condition).

forearm. Both of these are simple design parameters to control, without impacting the anchoring to the arm or the feasibility of the approach. Indeed, one fundamental feature of the proposed robot is the simplicity of the design and the inherently easy customization, together with a quick manufacturing procedure (within 10 min). For this study, we decided to use an unique actuator size for all the participants—as an initial test of the device's robustness; future work will customize actuator dimensions to individual anthropometry, ensuring an optimal fit and maximizing the effects.

After the ROM test, we asked the SCI individuals to play an exergame inducing forearm pronosupination for 2 min. The game consisted of a custom version of the classic Whac-A-Mole game, with four targets plus the baseline position calibrated for each patient and for each condition (*robot off, robot on*). Not only was the game positively appreciated by the participants compared to the ROM task—based on verbal feedback gathered during post session debriefings—but we were able to extract useful ad-hoc metrics automatically synchronized with the data from the sensors (kinematics from the IMU and muscular data from the EMG). Once again, the robot demonstrated its efficacy in supporting supination movements. We observed higher ROM (when assisted, all the targets were significantly more distant than

in the off condition) with no increase either in muscular activity, nor in the time to reach the target (at a group level, within 2 s despite the target), and a decrease in hold time (the time to spend over the target to score a point, especially for T4 and T5). Moreover, we measured an increase by 10% on the final score (number of hit moles) at the group level, with 6 out of 10 participants who increased their score and only 2 who reduced their score when assisted by the robot. Importantly, these two participants were able to achieve remarkable high scores (20 and 19, in line with 10 hits min^{-1} performed by the five healthy individuals on average) when not assisted, demonstrating their higher baseline condition compared to the rest of the group. While only validated on a videogame, these results are promising for future demonstrations in which participants will be tasked with real ADLs and object manipulation.

Our robot can provide up to 122 N of linear traction at only 70 kPa, with an estimated 2.2 Nm of maximum torque. Although this torque value is derived from the actuator's measured force–pressure behavior, it relies on a model that 1) treats the forearm as a rigid elliptical cylinder, 2) simplifies actuator action to tangential point forces along a uniformly wrapped helical path, and 3) neglects soft-tissue compliance, dynamic effects, and contact variability. Consequently, the estimate may overstate the true on-body torque—benchtop measurements often exceed in situ performance due to unmodeled interface dynamics[66]—and human–device interactions can further absorb part of the generated torque.[67] Nevertheless, this estimate provides a useful order of magnitude reference. Future work will incorporate direct in situ torque measurements to refine these estimates. Another pneumatic actuator,[44] which was evaluated in experiments with 6 healthy participants, required around 700 kPa to generate ≈1.7 Nm of torque, which was intentionally lowered down to 1.5 Nm because of mild discomfort reported during experimentation. The same research group reported a subsequent iteration of their design and tested it with 7 children with cerebral palsy,[45] showing improved weight (only 110 g) and lower maximum pressure (440 kPa) required to reach comparable torque to their previous version. In Das et al.[43] a couple of PAMs required more than 400 kPa to produce <15 N of linear force. These high-pressure values imply the need for stronger and thus bigger compressors, which are the weak point for any pneumatic technology targeting portability. Park et al.[47] showed a similar design (despite different anchoring location and air chamber shape), reaching up to 0.7 Nm at 50 kPa, but they did not validate their actuator with any human subjects. In another work, authors used shape memory alloys (SMA), producing 0.5 Nm to improve ROM by <20° in 4 stroke survivors.[46] However, this solution required a current of 1.5 A to heat the SMA coil springs, reaching up to 50 °C close to the skin (requiring serious risk mitigation strategies to avoid hazard), for a device weighing more than 1.5 kg (including a flexion actuator). Our solution is lightweight (30 g on the arm) and thin—about 20 mm when fully pressurized, comfortably below the discomfort threshold reported by Boser et al.[59]—while remaining safe and readily integrable with other technologies (e.g., robotic gloves) as the anchoring leaves the hand and the elbow unencumbered. While the presented design supports one direction of movement (either pronation or supination), depending on the anchoring, we produced an X-shaped version of the robot that is capable of simultaneously assisting both movements (pronation and supination) without requiring redonning of the actuator (see Figure S4a, Supporting Information).

Beyond the quantitative performance advantages outlined above, the real-world benefit of a wearable actuator ultimately depends on how reliably and comfortably it interfaces with the limb. Improper donning can degrade the performance of any wearable assistive device. In rigid exoskeletons, where precise joint alignment is paramount, even small misalignments can restrict the user's natural ROM, cause discomfort or injury, and dissipate the intended assistive torque at the human–device interface.[68–70] These challenges are not entirely eliminated in soft robotic systems;[67] however, the compliant fabrics used in such devices conform to the underlying anatomy, thereby accommodating for some degree of variability in fit and mitigating rigid-alignment issues.[71] In our textile actuator, the traction force is predominantly applied tangentially along the forearm because the fabric sleeve is anchored to the limb via the Velcro strap rather than through stiff, orthogonal linkages typical of rigid frames.[67] As Yandell et al.[67] noted, even in soft exosuits, a portion of assistive force can be dissipated through fabric stretch and slip at compliant interfaces; we addressed this by reinforcing the soft anchors along the major force paths. Moreover, the torques exchanged at this single DOF are considerably lower than those reported for rigid upper-limb exoskeletons, shifting the fitting challenge from user safety toward device efficiency—a topic we plan to examine further once the system is adapted for unsupervised use. Finally, weight, ease of donning–doffing, and reliable fit are recognized determinants of user acceptance.[71] Although the present study controlled these factors by having a trained researcher perform each donning procedure, future iterations could integrate color-coded alignment markers and dial-based quick-fit closures (i.e., BOA) to standardize the placement, enable one-handed self-donning, and further reduce the setup time; accompanying studies will quantify comfort and performance under these independent-use conditions.

From a control standpoint, the passive-triggered strategy, in which an IMU detects user-initiated motion, offers a simple, intuitive, and robust approach. Future iterations will implement more advanced solutions, including performance-adaptive strategies, that scale difficulty according to a participant's previous score and resistive modes that require the users to further engage with the actuator in a rehabilitation outlook. The inertial sensor can also be fused with other biosignals (e.g., surface EMG) to speed up the dynamics of the controller and accommodate participants with very limited residual volitational control. Beyond the controller, coupling the textile–pneumatic actuator with task-oriented virtual reality (VR) scenarios can deliver intensive, repetitive practice with real-time feedback—an approach shown to be feasible, safe, and at least as effective as conventional therapy in SCI cohorts.[72] Yet, only a handful of studies have combined VR with soft robotic devices, and these remain at a proof-of-concept stage,[73,74] leaving open the opportunity to demonstrate long-term benefits of modular, lightweight actuation. Unlike other conditions (i.e., multiple sclerosis)[75]—where robot-assisted VR training has driven measurable increases in functional performance—evidence for durable ADL transfer following VR training in SCI remains limited, underscoring the need for larger studies.[76,77]

As a preliminary investigation, we observed potential learning effects in two participants (S1 and S8) who were able to score enough points in each target location. They were indeed becoming faster in scoring a point while the game was proceeding. As this is an expected behavior, given the short familiarization time for the participant with both the robot and the exergame, in future work, we will need to better study this phenomenon as it could be used to optimally tune the difficulty of the game in a rehabilitation paradigm, to maximize engagement and thus, potentially rehabilitation.

This work represents a promising step further in the assistance of individuals suffering from neurological conditions, such as cervical SCI, using a soft wearable robot. While we discussed the need for multi-joint assistance, we only presented a single DOF robot, which clearly is a limitation of this work. However, as mentioned above, the thin and lightweight design potentially allows for seamless integration with other technologies. As proof of concept, Figure S4b, Supporting Information shows the integration of the pronosupination X-shaped module with a soft robot assisting the shoulder elevation on a healthy individual. Another limitation is linked to the sample size, with only 10 SCI individuals enrolled for the testing protocol. Confirmation of the results on a larger cohort and possibly on real ADLs would be necessary for strengthening our claims. Still, enrolling 10 SCI participants is inline or beyond the current state of the art for studies on soft wearables assisting any neurological population, in particular the few tackling SCI assistance.[7]

4. Experimental Section

The Robotic System: The robot was composed of a soft actuation module, a textile harness, an offboard controller, and an external laptop, running a custom graphical user interface. A video showing the donning and the working principle of the soft robot is available in the supplementary materials (Video S1, Supporting Information). The actuation module was made of TPU-coated nylon sheets (Ariatex, *DD Global Store*, Italy), heat pressed (160 °C, 170 s) together with a heat-resistant paper to form the air chamber. The actuator measured ≈0.11 L of volume. It was first attached distally to a neoprene hand brace with Velcro. It was then wrapped around the forearm and finally secured proximally—just above or below the elbow, depending on forearm length—using a Velcro strap sewn onto a custom neoprene armband (*DD Global Store*, Italy). Both the hand brace and the arm strap incorporated heat-bonded nylon-TPU reinforcements on the neoprene to prevent stretch along the load paths, thereby reducing loss of input power. See Figure S2, Supporting Information, for the design of the soft robot's air chamber, together with the soft anchoring and close-up views of the contractile units making up the air chamber. For this work, we saturated the pressure on the balloon to a maximum of 70 kPa to avoid any rupture.

The actuator was automatically controlled in pressure by a custom control box, including two air pumps (SP 622 EC-BL-DUp-DV, *Schwarzer Precision GmbH*, Germany), four miniature 2/2 normally closed solenoid valves (2x G068A319S1V00F3 ASCO, *Emerson Electric Co.*, USA, and 2x V2 model 14, *Parker*, USA), a miniature 2/2 normally closed solenoid valve for the pump exhaust (LVM10R3, *SMC Corporation*, Japan), a microcontroller (Feather M4 Express, *Adafruit*, USA), and custom electronics (see Supplementary Figure S3, Supporting Information). The portable benchtop control box weighed 2.1 kg, measured $22 \times 14 \times 30$ cm, was wall-powered, and produced 52.0 dB of ambient noise—peaking at 57.5 dB when the pumps were active. Noise measurements were taken with a sound level meter (72-942, Multicomp Pro, USA) in a 42 dB noise environment, placing the system's acoustic emissions within the range of a normal conversation.[78] The microcontroller ran a low-level pressure control loop (bang–bang with hysteresis) at 200 Hz, measuring the pressure in the actuators via pressure sensors (ABPDANV060PGAA5, *Honeywell International Inc.*, USA). At the higher level, user intention was detected via an IMU mounted on the forearm. The high-level controller implemented a passive-triggered strategy. When the participant began moving toward the target angle, the IMU detected the intention once the forearm angular velocity crossed an adjustable threshold that was tuned to the participant's residual motor capacity. After this trigger, the controller inflates, holds, or vents the actuator according to the real-time forearm angle—shown as a cursor on the monitor—relative to the target angle, thereby supplying assistance until the point is scored in the exergame.

The graphical user interface runs a custom version of the classic game Whac-A-Mole. A simple target-hitting task was selected to minimize cognitive load and isolate the functional effect of the pronosupination assistance, while still providing an engaging, quantitatively scored benchmark. The game was programmed in MATLAB2024a (*MathWorks*, USA) using real-time information from the IMU (supination angle θ) to move the cursor (a hammer) horizontally over the targets (dens). Starting from a resting position (T1, $\theta = 0$), to score a point (hitting the mole), the cursor needs to reach the target (time to target) and then hold in position (hold time) for a minimum of 1 s. A vertical bar shows the elapsed time over the target. If the cursor exits from an allowed range ($|\theta| < \theta_{\text{range}}$, where θ_{range} is 2.5% of the target angle), the hold time restarts. In the assisted condition, depending on the position of the cursor with respect to the target, the interface sends, via serial port, the input to the pressure control loop in the soft robot control box. Once a point is scored, the actuator vents to allow the participant to return to the resting position, after which a new target is presented.

Mechanical Characterization Protocol: The mechanical response of the actuator was characterized by measuring its geometric and force-generation properties under controlled conditions. First, the actuator length was measured when unpowered (L_{off}, 0 kPa) and fully powered (L_{on}, 70 kPa). The resulting overall CR was used as a parameter in the subsequent stage of mechanical characterization. Isometric tests were then conducted with the actuator securely clamped within a universal testing machine (Instron 5965, *Instron Corporation*, USA) between a 1 kN load cell and the base plate. The CR was incrementally stepped from 0% to 100% by increments of 10%. For each CR, the supplied pressure was varied from 0 to 70 kPa by steps of 7 kPa, and the corresponding force was recorded using the load cell.

Human Testing Protocol: A total of 15 individuals (5 healthy and 10 SCI) voluntarily joined a single-session study protocol. Informed consent was obtained by each of them prior to participation. Data collection on the healthy participants took place at the Biorobotics Institute of Scuola Superiore Sant'Anna, Pontedera (PI), Italy, after approval of the testing protocol (32/2023, 01/2024) by the Joint Ethics Committee of the Scuola Normale Superiore and the Scuola Superiore Sant'Anna. Data collection on the SCI participants, instead, took place at the Careggi University Hospital, Florence, Italy, after approval of the testing protocol (35/2022) by the Politecnico of Milan review board.

For all the testing conditions and participants, we measured EMG activity with surface wet electrodes (Sessantaquattro+, *OT Bioelettronica s.r.l.*, Italy) in two muscles of the arm, respectively the biceps and the pronator teres. Sensor placement was determined according to the recommendations on surface EMG for the noninvasive assessment of muscle activity.[79] EMG data was sampled at 2 kHz, then bandpass-filtered (fourth order, 10–400 Hz), rectified, and lastly lowpass-filtered (fourth order, 10 Hz). In the healthy cohort, MVC was measured for each muscle as the mean value of the maximum EMG across three consecutive isometric contractions performed while participants held a cylinder fixed on a firm support, which provided resistance to their pronation or supination motion. Normalized EMG was then computed to allow inter-subject comparison. On the contrary, in the patient cohort, the MVC was not performed due to the excessively fatiguing nature of the task for these individuals. In this case, instead, the maximum contraction value for each muscle across the whole testing session was used as MVC and then normalized for inter-subject comparison. Moreover, we measured forearm kinematics using one IMU (MTw Awinda, *Movella XSens*, The Netherlands), following a standard sensor calibration routine. Kinematic data was sampled at 200 Hz and lowpass-filtered by means of a complementary filter (smoothing factor 0.7). All the tests were recorded with a camera for documentary purposes (Hero10, *GoPro*, USA).

The testing protocol with the healthy participants consisted of two consequent exercises. First, in the mechanical transparency test, the two following conditions were evaluated and randomized among participants: device not worn (*no robot*) and device donned and powered off (*robot off*). For the robot-off condition, a member of the research team fitted the device to the participant's dominant forearm while the participant kept the limb relaxed; no fine arm or hand movements were required. A brief familiarization session then followed, covering the actuation mechanism and control strategy. During this familiarization, the device's pressure was gradually increased toward the set saturation limit of 70 kPa or stopped sooner if the participant reported any discomfort. Importantly, no participants required the pressure to be limited below 70 kPa due to discomfort or any other reason. The set pressure (70 kPa) was then used as the upper limit for subsequent tasks; because this value was never exceeded, participant comfort was assumed to be safeguarded for the entire session. In each transparency condition, starting from a rest position (forearm fully pronated), participants were asked three times to supinate to their max supination angle. After a 10-min break, participants were asked to perform 2-min exergame sessions aimed at providing a reference about the hit count, to be compared with observations from the SCI patients. The target-hitting exergame (Whac-A-Mole) was played in the two following conditions, randomized among participants: robot donned and powered off (*robot off*), robot donned and powered on (*robot on*). The target presentation order was randomized as well. The score was not shown in real-time in order not to bias the participants' performance.

The testing protocol with the SCI participants was similar to the one carried out with the healthy individuals. The same donning, familiarization, and safety-pressure procedure was applied by a research team member. Then, participants were asked to perform a maximum ROM task. Starting from a rest position, they were asked to supinate to their max supination angle for three times in both, *robot off* and *robot on* conditions (randomized among participants). Max ROM data from this test was used to calibrate the targets for the game (T5 = max ROM, the other equally spaced with respect to the baseline and T5) in both, *robot off* and *robot on* conditions. After a 10-min break between the tests, to avoid excessive fatigue, participants were engaged in achieving their maximum score at the target-hitting game for a total of 2 min. Again, the score was not shown in order not to bias their performance. Two conditions (*assisted* vs. *unassisted*) were randomized between subjects, and were separated by a 10-min break. Moreover, the 4 targets were also randomized within each session. The protocol ended after playing the exergame in both conditions, and the participants doffed the robot with the help of the research team.

Statistical Analysis: Given the small sample size, a Wilcoxon signed-rank test was used to compare the conditions (no robot versus robot off for the transparency tests with healthy participants, robot off versus robot on with the SCI participants). The significance level was reported when exceeding the standard *p*-value of significance ($p < 0.05$, marked with a single asterisk *, $p < 0.01$, marked with two asterisks **). The analysis was performed on MATLAB.

Supporting Information

Supporting Information is available from the Wiley Online Library or from the author.

Acknowledgements

The authors would like to thank all the participants who volunteered in this study.

Open access publishing facilitated by Scuola Superiore Sant'Anna, as part of the Wiley - CRUI-CARE agreement.

Conflict of Interest

The authors declare no conflict of interest.

Author Contributions

Tommaso Proietti and **Roberto Ferroni** built the robot (textile, mechatronics, and software). **Tommaso Proietti**, **Roberto Ferroni**, **Gaetano D'Avola**, and **Silvestro Micera** developed the study protocol. **Roberto Ferroni**, **Gaetano D'Avola**, **Daniele Filippo Mauceri**, **Chiara Pau**, and **Giorgia Sciarrone** ran the protocol. **Roberto Ferroni** processed the data and ran statistical analysis. **Tommaso Proietti**, **Roberto Ferroni**, and **Silvestro Micera** wrote the original manuscript. All authors reviewed the manuscript and provided critical feedback. **Silvestro Micera** and **Tommaso Proietti** contributed equally to this work.

Data Availability Statement

The data that support the findings of this study are available in the supplementary material of this article.

Keywords

assistive technology, rehabilitation robotics, soft robotics, spinal cord injuries, wearable robotics

Received: January 28, 2025
Revised: May 30, 2025
Published online:

[1] X. Hu, W. Xu, Y. Ren, Z. Wang, X. He, R. Huang, B. Ma, J. Zhao, R. Zhu, L. Cheng, *Signal Transduction Targeted Ther.* **2023**, *8*, 245.
[2] Y. Lu, Z. Shang, W. Zhang, M. Pang, X. Hu, Y. Dai, R. Shen, Y. Wu, C. Liu, T. Luo, X. Wang, B. Liu, L. Zhang, L. Rong, *BMC Med.* **2024**, *22*, 285.
[3] K. D. Anderson, *J. Neurotrauma* **2004**, *21*, 1371.
[4] W. Tigra, M. Dali, L. William, C. Fattal, A. Gélis, J. L. Divoux, B. Coulet, J. Teissier, D. Guiraud, C. Azevedo Coste, *J. NeuroEngineering Rehabil.* **2020**, *17*, 66.
[5] C. Azevedo Coste, L. William, L. Fonseca, A. Hiairrassary, D. Andreu, A. Geffrier, J. Teissier, C. Fattal, D. Guiraud, *Sci. Rep.* **2022**, *12*, 16189.
[6] N. Dunkelberger, E. M. Schearer, M. K. O'Malley, *Exp. Neurol.* **2020**, *328*, 113274.
[7] T. Proietti, E. Ambrosini, A. Pedrocchi, S. Micera, *IEEE Access* **2022**, *10*, 106117.
[8] S. R. Soekadar, M. Witkowski, N. Vitiello, N. Birbaumer, *Biomed. Eng. Biomed. Tech.* **2015**, *60*, 199.
[9] L. Randazzo, I. Iturrate, S. Perdikis, J. D. R. Millan, *IEEE Robot. Autom. Lett.* **2018**, *3*, 500.
[10] C. Correia, K. Nuckols, D. Wagner, Y. M. Zhou, M. Clarke, D. Orzel, R. Solinsky, S. Paganoni, C. J. Walsh, *IEEE Trans. Neural Syst. Rehabil. Eng.* **2020**, *28*, 1407.
[11] T. Bützer, O. Lambercy, J. Arata, R. Gassert, *Soft Robot.* **2021**, *8*, 128.
[12] S. Hesse, H. Schmidt, C. Werner, *J. Rehabil. Res. Dev.* **2006**, *43*, 671.
[13] V. Squeri, L. Masia, P. Giannoni, G. Sandini, P. Morasso, *IEEE Trans. Neural Syst. Rehabil. Eng.* **2014**, *22*, 312.
[14] T. L. Zhu, J. Klein, S. A. Dual, T. C. Leong, E. Burdet, in *2014 IEEE/RSJ Int. Conf. on Intelligent Robots and Systems*, IEEE, Chicago, IL **2014**, pp. 2107–2113, https://doi.org/10.1109/IROS.2014.6942845.
[15] K. X. Khor, P. J. H. Chin, C. F. Yeong, E. L. M. Su, A. L. T. Narayanan, H. A. Rahman, Q. I. Khan, *IEEE Trans. Neural Syst. Rehabil. Eng.* **2017**, *25*, 1864.
[16] A. Nehrujee, H. Andrew, Reethajanetsurekha, A. Patricia, S. Samuelkamaleshkumar, H. Prakash, S. Sujatha, S. Balasubramanian, *IEEE Access* **2021**, *9*, 134957.

[17] G. R. Johnson, D. A. Carus, G. Parrini, S. S. Marchese, R. Valeggi, *Proc. Inst. Mech. Eng.* **2001**, *215*, 275.
[18] R. A. R. C. Gopura, K. Kiguchi, *J. Natl. Sci. Found. Sri Lanka* **2009**, *37*, 241.
[19] T. M. Kwok, H. Yu, *IEEE Trans. Neural Syst. Rehabil. Eng.* **2024**, *32*, 3299.
[20] S. Hesse, G. Schulte-Tigges, M. Konrad, A. Bardeleben, C. Werner, *Arch. Phys. Med. Rehabil.* **2003**, *84*, 915.
[21] Y. Hsieh, C. Wu, W. Liao, K. Lin, K. Wu, C. Lee, *Neurorehabilitation Neural Repair* **2011**, *25*, 503.
[22] M. Gandolfi, E. Formaggio, C. Geroin, S. F. Storti, I. Boscolo Galazzo, M. Bortolami, L. Saltuari, A. Picelli, A. Waldner, P. Manganotti, N. Smania, *Neural Plast.* **2018**, *2018*, 1.
[23] O. Lambercy, L. Dovat, H. Yun, S. K. Wee, C. W. K. Kuah, K. S. G. Chua, R. Gassert, T. E. Milner, C. L. Teo, E. Burdet, *J. NeuroEngineering Rehabil.* **2011**, *8*, 63.
[24] K. K. Ang, C. Guan, K. S.Phua, C. Wang, L. Zhou, K. Y. Tang, G. J. E. Joseph, C. W. K. Kuah, K. S. G. Chua, *Front. Neuroeng.* **2014**, *7*, 30.
[25] L. Masia, M. Casadio, P. Giannoni, G. Sandini, P. Morasso, *J. NeuroEngineering Rehabil.* **2009**, *6*, 44.
[26] C. F. Yeong, K. Baker, A. Melendez-Calderon, E. Burdet, E. D. Playford, in *2010 IEEE Conf. on Robotics, Automation and Mechatronics*, IEEE, Singapore **2010**, pp. 90–95, https://doi.org/10.1109/RAMECH.2010.5513206.
[27] S. Mazzoleni, V.-D. Tran, P. Dario, F. Posteraro, *IEEE Trans. Neural Syst. Rehabil. Eng.* **2019**, *27*, 1458.
[28] A. Picelli, S. Tamburin, M. Passuello, A. Waldner, N. Smania, *J. NeuroEngineering Rehabil.* **2014**, *11*, 28.
[29] G. G. Fluet, Q. Qiu, D. Kelly, H. D. Parikh, D. Ramirez, S. Saleh, S. V. Adamovich, *Dev. Neurorehabilitation* **2010**, *13*, 335.
[30] L. Z. Tong, J. Klein, S. A. Dual, T. C. Leong, E. Burdet, in *2015 37th Annual Int. Conf. of the IEEE Engineering in Medicine and Biology Society (EMBC)*, IEEE, Milan **2015**, pp. 3933–3936, https://doi.org/10.1109/EMBC.2015.7319254.
[31] N. Yozbatiran, J. Berliner, C. Boake, M. K. O'Malley, Z. Kadivar, G. E. Francisco, in *2011 IEEE Int. Conf. on Rehabilitation Robotics*, IEEE, Zurich **2011**, pp. 1–4, https://doi.org/10.1109/ICORR.2011.5975425.
[32] N. Yozbatiran, J. Berliner, M. K. O'Malley, A. U. Pehlivan, Z. Kadivar, C. Boake, G. E. Francisco, *J. Rehabil. Med.* **2012**, *44*, 186.
[33] N. Dunkelberger, S. A. Carlson, J. Berning, E. M. Schearer, M. K. O'Malley, *IEEE Trans. Neural Syst. Rehabil. Eng.* **2024**, *32*, 956.
[34] J. Chen, P. S. Lum, *J. NeuroEngineering Rehabil.* **2018**, *15*, 13.
[35] J. M. Catalán, E. Trigili, M. Nann, A. Blanco-Ivorra, C. Lauretti, F. Cordella, E. Ivorra, E. Armstrong, S. Crea, M. Alcañiz, L. Zollo, S. R. Soekadar, N. Vitiello, N. García-Aracil, *J. NeuroEngineering Rehabil.* **2023**, *20*, 61.
[36] X. Zhang, M. Wang, H. Wang, F. Wang, L. Chen, W. Mu, J. Wang, X. Kang, *IEEE Trans. Neural Syst. Rehabil. Eng.* **2023**, *31*, 2665.
[37] S. R. Soekadar, M. Witkowski, C. Gómez, E. Opisso, J. Medina, M. Cortese, M. Cempini, M. C. Carrozza, L. G. Cohen, N. Birbaumer, N. Vitiello, *Sci. Robot.* **2016**, *1*, eaag3296.
[38] U. Mayetin, S. Kucuk, *J. Intell. Robot. Syst.* **2022**, *106*, 65.
[39] R. A. R. C. Gopura, K. Kiguchi, in *2007 Int. Conf. on Industrial and Information Systems*, IEEE, Peradeniya, Sri Lanka **2007**, pp. 535–540, https://doi.org/10.1109/ICIINFS.2007.4579235.
[40] H. Su, K.-S. Lee, Y. Kim, H.-S. Park, *IEEE Robot. Autom. Lett.* **2022**, *7*, 12078.
[41] H. Su, F. Missiroli, X. Zhang, C. Becchio, H.-S. Park, L. Masia, in *2024 10th IEEE RAS/EMBS Int. Conf. for Biomedical Robotics and Biomechatronics (BioRob)*, IEEE, Heidelberg, Germany **2024**, pp. 1011–1016, https://doi.org/10.1109/BioRob60516.2024.10719915.
[42] S. Balasubramanian, R. Wei, M. Perez, B. Shepard, E. Koeneman, J. Koeneman, J. He, in *2008 Virtual Rehabilitation*, IEEE, Vancouver, BC **2008**, pp. 163–167, https://doi.org/10.1109/ICVR.2008.4625154.
[43] S. Das, Y. Kishishita, T. Tsuji, C. Lowell, K. Ogawa, Y. Kurita, *IEEE Robot. Autom. Lett.* **2018**, *3*, 2416.
[44] J. Realmuto, T. Sanger, in *2019 2nd IEEE Int. Conf. on Soft Robotics (RoboSoft)*, IEEE, Seoul, Korea (South) **2019**, pp. 591–596, https://doi.org/10.1109/ROBOSOFT.2019.8722759.
[45] J. Realmuto, T. D. Sanger, *Front. Robot. AI* **2022**, *9*, 877041.
[46] J. Jeong, K. Hyeon, S.-Y. Jang, C. Chung, S. Hussain, S.-Y. Ahn, S.-K. Bok, K.-U. Kyung, *IEEE Robot. Autom. Lett.* **2022**, *7*, 6028.
[47] S.-H. Park, J. Yi, D. Kim, Y. Lee, H. S. Koo, Y.-L. Park, in *2019 2nd IEEE Int. Conf. on Soft Robotics (RoboSoft)*, IEEE, Seoul, Korea (South) **2019**, pp. 636–641, https://doi.org/10.1109/ROBOSOFT.2019.8722783.
[48] S. Jacobson, E. M. Marcus, *Neuroanatomy for the Neuroscientist*, Springer US, Boston, MA **2011**, https://doi.org/10.1007/978-1-4419-9653-4.
[49] P. Staubli, T. Nef, V. Klamroth-Marganska, R. Riener, *J. NeuroEngineering Rehabil.* **2009**, *6*, 46.
[50] J. Allington, S. J. Spencer, J. Klein, M. Buell, D. J. Reinkensmeyer, J. Bobrow, in *2011 Annual Int. Conf. of the IEEE Engineering in Medicine and Biology Society*, IEEE, Boston, MA **2011**, pp. 1579–1582, https://doi.org/10.1109/IEMBS.2011.6090459.
[51] J. A. French, C. G. Rose, M. K. O'Malley, in *Volume 3: Industrial Applications; Modeling for Oil and Gas, Control and Validation, Estimation, and Control of Automotive Systems; Multi-Agent and Networked Systems; Control System Design; Physical Human-Robot Interaction; Rehabilitation Robotics; Sensing and Actuation for Control; Biomedical Systems; Time Delay Systems and Stability; Unmanned Ground and Surface Robotics; Vehicle Motion Controls; Vibration Analysis and Isolation; Vibration and Control for Energy Harvesting; Wind Energy*, American Society of Mechanical Engineers, San Antonio, TX **2014**, p. V003T43A006, https://doi.org/10.1115/DSCC2014-6267.
[52] D. Buongiorno, E. Sotgiu, D. Leonardis, S. Marcheschi, M. Solazzi, A. Frisoli, *IEEE Robot. Autom. Lett.* **2018**, *3*, 2152.
[53] H. I. Krebs, B. T. Volpe, D. Williams, J. Celestino, S. K. Charles, D. Lynch, N. Hogan, *IEEE Trans. Neural Syst. Rehabil. Eng.* **2007**, *15*, 327.
[54] M. Atlihan, E. Akdogan, M. S. Arslan, in *2014 19th Int. Conf. on Methods and Models in Automation and Robotics (MMAR)*, IEEE, Miedzyzdroje **2014**, pp. 52–57, https://doi.org/10.1109/MMAR.2014.6957324.
[55] J. A. Martinez, P. Ng, Son Lu, M. S. Campagna, O. Celik, in *2013 IEEE 13th Int. Conf. on Rehabilitation Robotics (ICORR)*, IEEE, Seattle, WA **2013**, pp. 1–6, https://doi.org/10.1109/ICORR.2013.6650459.
[56] M.-H. Milot, S. J. Spencer, V. Chan, J. P. Allington, J. Klein, C. Chou, J. E. Bobrow, S. C. Cramer, D. J. Reinkensmeyer, *J. NeuroEngineering Rehabil.* **2013**, *10*, 112.
[57] A. U. Pehlivan, F. Sergi, A. Erwin, N. Yozbatiran, G. E. Francisco, M. K. O'Malley, *Robotica* **2014**, *32*, 1415.
[58] Hang Zhang, H. Austin, S. Buchanan, R. Herman, J. Koeneman, J. He, in *2011 IEEE Int. Conf. on Rehabilitation Robotics*, IEEE, Zurich **2011**, pp. 1–6, https://doi.org/10.1109/ICORR.2011.5975440.
[59] Q. A. Boser, M. R. Dawson, J. S. Schofield, G. Y. Dziwenko, J. S. Hebert, *Prosthet. Orthot. Int.* **2021**, *45*, 161.
[60] S. Lessard, P. Pansodtee, A. Robbins, J. M. Trombadore, S. Kurniawan, M. Teodorescu, *IEEE Trans. Neural Syst. Rehabil. Eng.* **2018**, *26*, 1604.
[61] L. Gerez, S. Micera, R. Nuckols, T. Proietti, *Curr. Opin. Neurol.* **2024**, *37*, 645.

[62] N. Lotti, F. Missiroli, E. Galofaro, E. Tricomi, D. Di Domenico, M. Semprini, M. Casadio, G. Brichetto, L. De Michieli, A. Tacchino, L. Masia, *Soft Robot.* **2024**, *11*, 338.
[63] T. Proietti, A. Bandini, *IEEE Trans. Neural Syst. Rehabil. Eng.* **2024**, *32*, 2737.
[64] P. V. Fulton, S. Lohlein, N. Paredes-Acuna, N. Berberich, G. Cheng, in *2021 20th Int. Conf. on Advanced Robotics (ICAR)*, IEEE, Ljubljana, Slovenia **2021**, pp. 575–580, https://doi.org/10.1109/ICAR53236.2021.9659397.
[65] A. Sinha, M. A. Nazar, J. Moorehead, V. Bhalaik, P. Brownson, *Shoulder Elbow* **2010**, *2*, 118.
[66] C. M. McCann, C. J. Hohimer, C. T. O'Neill, H. T. Young, K. Bertoldi, C. J. Walsh, *IEEE Trans. Med. Robot. Bionics* **2023**, *5*, 363.
[67] M. B. Yandell, B. T. Quinlivan, D. Popov, C. Walsh, K. E. Zelik, *J. NeuroEngineering Rehabil.* **2017**, *14*, 40.
[68] M. B. Näf, K. Junius, M. Rossini, C. Rodriguez-Guerrero, B. Vanderborght, D. Lefeber, *Appl. Mech. Rev.* **2018**, *70*, 050802.
[69] R. Mallat, M. Khalil, G. Venture, V. Bonnet, S. Mohammed, in *2019 Fifth Int. Conf. on Advances in Biomedical Engineering (ICABME)*, IEEE, Tripoli, Lebanon **2019**, pp. 1–4, https://doi.org/10.1109/ICABME47164.2019.8940321.
[70] N. Jarrasse, G. Morel, *IEEE Trans. Robot.* **2012**, *28*, 697.
[71] J. Chung, D. A. Quirk, M. Applegate, M. Rouleau, N. Degenhardt, I. Galiana, D. Dalton, L. N. Awad, C. J. Walsh, *Commun. Eng.* **2024**, *3*, 35.
[72] M. Scalise, T. S. Bora, C. Zancanella, A. Safa, R. Stefini, D. Cannizzaro, *J. Clin. Med.* **2024**, *13*, 5429.
[73] P. Tran, S. Jeong, F. Lyu, K. Herrin, S. Bhatia, D. Elliott, S. Kozin, J. P. Desai, *IEEEASME Trans. Mechatron.* **2022**, *27*, 3920.
[74] F. Li, J. Chen, G. Ye, S. Dong, Z. Gao, Y. Zhou, *Biomimetics* **2023**, *8*, 83.
[75] D. Gijbels, I. Lamers, L. Kerkhofs, G. Alders, E. Knippenberg, P. Feys, *J. NeuroEngineering Rehabil.* **2011**, *8*, 5.
[76] S. Prasad, R. Aikat, S. Labani, N. Khanna, *Asian Spine J.* **2018**, *12*, 927.
[77] I. Dimbwadyo-Terrer, A. Gil-Agudo, A. Segura-Fragoso, A. de los Reyes-Guzmán, F. Trincado-Alonso, S. Piazza, B. Polonio-López, *BioMed Res. Int.* **2016**, *2016*, 1.
[78] B. Berglund, T. Lindvall, D. H. Schwela, *Noise Vib. Worldw.* **2000**, *31*, 24.
[79] Sensor Locations, *Recommendations for sensor locations on individual muscles* http://seniam.org/sensor_location.htm.